Aptamers ISSN: 2514-3247 Aptamers, 2017, Vol 1, 13–18

MINI-REVIEW

NMR study of aptamers

Taiichi Sakamoto

Department of Life Science, Faculty of Advanced Engineering, Chiba Institute of Technology, 2-17-1 Tsudanuma, Narashino-shi, Chiba 275-0016, Japan

Correspondence to: Email: taiichi.sakamoto@p.chibakoudai.jp

Received: 18 October 2017 | Revised: 11 November 2017 | Accepted: 11 November 2017 | Published: 11 November 2017

ABSTRACT

Nuclear magnetic resonance spectroscopy is a powerful technique that helps to determine the structures of biomolecules. Since the 1980s when nuclear magnetic resonance began to be applied in the determination of nucleic acid structures, it has been used to study aptamer structures and aptamer–target interactions. Nuclear magnetic resonance spectroscopy has revealed that aptamers adopt characteristic conformations and bind specifically to their targets. It is not easy to determine the structure of aptamers by nuclear magnetic resonance, especially in the case of aptamer–large target molecule complexes. However, nuclear magnetic resonance provides useful information about aptamers, even when their structure cannot be determined. This review includes the studies in which nuclear magnetic resonance spectroscopy was employed recently to analyse aptamers in several ways in addition to analysing them for structure determination.

KEYWORDS: Nuclear magnetic resonance, aptamer, tertiary structure, interaction, secondary structure

INTRODUCTION

Aptamers are single-stranded oligonucleotides that often exhibit high affinity for and specificity to their target molecules, which could be peptides, proteins, whole cells or small molecules (e.g., nucleotides and amino acids). Aptamers are selected from large pools of randomized oligonucleotide libraries (approximately 10^{15} variants) by Systematic Evolution of Ligands by Exponential Enrichment (SELEX) (Darmostuk et al, 2015). Because of their high specificity for and affinity to their target molecules, similar to an antibody binding to its antigen, aptamers could be used as research reagents and in diagnostics and therapeutics. The binding of an aptamer to its target depends on the nature of the target and on the nucleotide sequence and 3D structure of the aptamer; therefore, structural and biophysical studies are necessary to understand the cause of the high affinity and specificity and would accelerate the use of aptamers in research, diagnostics and therapeutics.

X-ray crystallography and nuclear magnetic resonance (NMR) spectroscopy have been used to study the three-dimensional structures of biomolecules. Each method has its advantages and limitations. Determination of high-resolution structures using NMR spectroscopy is limited to relatively small molecules (<30-40 kDa) because of the overlap and broadening of NMR signals. On the other hand, structures of arbitrarily large molecules can be determined by X-ray crystallography, but only if the crystals provide suitable quality of diffraction data. Indeed, a significant degree of trial and error is still required to determine the conditions that yield well-diffracting crystals (Chayen and Saridakis, 2008). Furthermore, crystallization of oligonucleotides is usually more difficult than that of proteins. Therefore, the structures of many aptamers, which lie within the 30–50-mer range and bind to small target molecules, have been determined using NMR. On the other hand, the crystal structures of aptamer–large target molecule complexes have been determined by X-ray crystallography (Nomura et al, 2010; Gelinas et al, 2016; Bjerregaard et al, 2016).

NMR analysis, like X-ray crystallography, usually requires a large amount of sample; however, it does not require

crystallization. Therefore, NMR signals that contain structural information can be obtained quickly, although it takes a significant amount of time to analyse them in order to determine the structure. This review includes the studies in which NMR spectroscopy was employed recently to analyse aptamers in several ways in addition to analysing them for structure determination.

SOLUTION STRUCTURE DETERMINATION

The sequential assignment of NMR signals using $^{13}C/^{15}N$-labelled protein and triple-resonance experiments is an already established method. Moreover, the entire process, from signal assignment to structure determination, is automated. However, the determination of nucleic acid structure using $^{13}C/^{15}N$-labelled nucleic acid and heteronuclear multidimensional NMR, which was developed in the early 1990s, is still under development (Barnwal et al, 2017). Therefore, in the 1990s, NMR spectroscopy was used to determine the aptamer structures with a range of ligands including the cofactors ATP (Dieckmann et al, 1996; Jiang et al, 1996) and FMN (Fan et al, 1996), the amino acids L-arginine and L-citrulline (Yang et al, 1996), and the aminoglycoside antibiotic tobramycin (Jiang et al, 1997b) (Table 1); NMR spectroscopy was successfully applied in the determination of these structures as the RNA conformations were fixed in defined compact conformations when bound to high-affinity ligands, resulting in analysable narrow NMR signals.

The structure determination of aptamer–protein complexes using NMR spectroscopy is not easy due to signal broadening; therefore, free-form structures have been determined for those aptamers whose targets are proteins. Comparisons of unbound-form aptamer structures with their bound–form structures, determined by X-ray crystallography, revealed that the conformation of aptamers changed upon binding, although only two cases has been reported to date (Figure 1A and B) (Huang et al, 2003; Reiter et al, 2008; Davlieva et al, 2014); however, no such conformational change was observed in the target proteins involved (Bjerregaard et al, 2016; Gelinas et al, 2016). These structural comparisons between free and bound forms reveal that aptamers undergo an induced fit upon binding to target proteins and exhibit great plasticity in terms of accommodating the optimal conformations required for complex formation.

However, one interesting example of an aptamer whose conformation remained almost unchanged upon peptide binding was provided by Mashima and colleagues who reported that the anti-prion aptamer folded into a unique

Table 1. NMR structures of aptamers[a].

Target	Free or complex	DNA or RNA	Author, year
thrombin	free	DNA	Schultze et al, 1994 Marathias et al, 1996
FMN	complex	RNA	Fan et al, 1996
L-arginine	complex	RNA	Yang et al, 1996
L-citrulline	complex	RNA	Yang et al, 1996
ATP	complex (AMP)[b]	RNA	Dieckmann et al, 1996 Jiang et al, 1996
ATP	complex (AMP)	DNA	Lin et al, 1997
HIV-1 Rev peptide	complex	RNA	Ye et al, 1996
tobramycin	complex	RNA	Jiang et al, 1997
L-arginineamide	complex	DNA	Lin et al, 1998 Robertson et al, 2000
neomycin B	complex	RNA	Jiang et al, 1999
HTLV-1 Rex peptide	complex	RNA	Jiang et al, 1999
HIV-1 Tat protein	complex (L-arginineamide)	RNA	Matsugami et al, 2003
malachite green	complex	RNA	Flinders et al, 2004
eIF4A	free (partial)	RNA	Sakamoto et al, 2005
GTP	complex	RNA	Carothers et al, 2006
TAR RNA	complex	modified nucleic acid	Lebars et al, 2007
NF-κB	free	RNA	Reiter et al, 2008
TAR RNA	complex	RNA	Van Melckebeke et al, 2008
bovine prion	free	RNA	Mashima et al, 2009
mucin 1	free	DNA	Baouendi et al, 2012
AML1 Runt domain	free (partial)	RNA	Nomura et al, 2013
bovine prion	complex (peptide)	RNA	Mashima et al, 2013
VEFG	free	modified nucleic acid	Marušič et al, 2013
ribosomal protein S8	free	RNA	Davlieva et al, 2014
GTP	complex	RNA	Wolter et al, 2017
thrombin	free	modified nucleic acid	Lietard et al, 2017

[a]Only aptamers obtained by SELEX are listed.
[b]In parentheses, the complex partner or the partial structure, in the case of free form structures.

quadruplex structure in both the free and peptide-bound forms (Figure 1C) (Mashima et al, 2009; Mashima et al, 2013). In the structures, the aptamer formed a dimer and each monomer simultaneously bound itself to two portions of the N-terminal peptide of the prion protein. In this case, it was the disordered peptide that underwent an induced fit to the rigid quadruplex structure of the aptamer.

SECONDARY STRUCTURE ANALYSIS

Tertiary structure determination of nucleic acids is complicated when there is a high degree of overlap between signals. However, imino proton signals of guanosine, uridine and thymidine residues are observed between 10 and -15ppm and resolve well compared with other signals, and these imino proton signals provide valuable information about base pairing in nucleic acid molecules. These signals are observable when the imino protons are involved in hydrogen bonding or are protected from exchange with bulk solvent water. Thus, Watson–Crick base pairs (G–C, A–U and A–T), non-Watson–Crick base pairs (e.g. G–U or G–A), and G-quartets are detected by analysing the imino proton spectrum of nucleic acid. Analysis of the exchange rate of imino protons could provide more quantitative information about the stability of base pairing (Churcher et al, 2017).

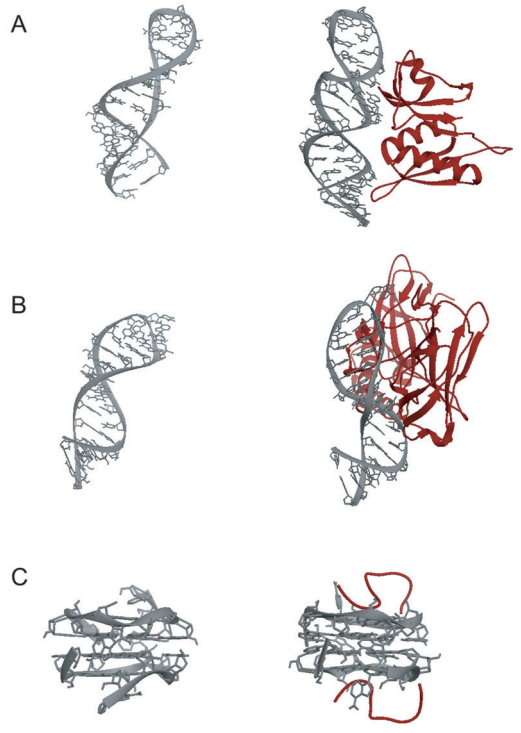

Figure 1. Conformational change of aptamers upon protein binding. (A) NMR structure of the free S8 aptamer (left; PDB ID 2LUN) and crystal structure of the S8-aptamer complex (right; PDB ID 4PDB). (B) NMR structure of the free NF-kB aptamer (left; PDB ID 2JWV) and crystal structure of the NF-kB-aptamer complex (right; PDB ID 1OOA). (C) NMR structure of the free prion aptamer (left; PDB ID 2RQJ) and NMR structure of the prion peptide-aptamer complex (right; PDB ID 2RSK). Aptamers are shown in grey, with the protein or peptide backbones in red. This figure was created using UCSF Chimera (Pettersen et al, 2004).

Increasing the sample temperature causes denaturation of the nucleic acid conformation, resulting in the disappearance of the imino proton signals. Therefore, analyses of imino proton signals at different temperatures provide information about the thermal stability of the aptamer. In the case of the aptamer against salivary α-amylase, in which (*E*)-5-(2-(*N*-(2-(N6-adeninyl)ethyl))carbamylvinyl)-2′-deoxyuridine-5′-triphosphate (dU^{ad}TP) is incorporated instead of thymidine-5′-triphosphate (TTP), imino proton spectra analysis at different temperatures indicated that the aptamer adopts a defined structure and is stable at 40°C although the signals could not be assigned due to the overlapping and broadening (Figure 2) (Minagawa et al, 2017). Furthermore, the H9N9 imino proton signals of the adenine component of U^{ad} were observed in this case. If these signals could be assigned, these could be a good probe to analyse the local structure of the aptamer.

INTERACTION ANALYSIS

Crystal structures of aptamer–target complexes provide precise information on their interactions. However, crystalizing aptamers or aptamer–target complexes is difficult, and only a few co-crystal structures have been reported over the years. With the availability of target protein structure coordinates, interaction analysis using NMR may represent a good approach to elucidating the aptamer binding surface.

In the case of an IgG aptamer, chemical shift perturbation analysis of the IgG Fc fragment upon aptamer binding was used to determine the binding surface of the Fc fragment (Miyakawa et al, 2008). Figure 3A shows the ^{1}H-^{15}N HSQC

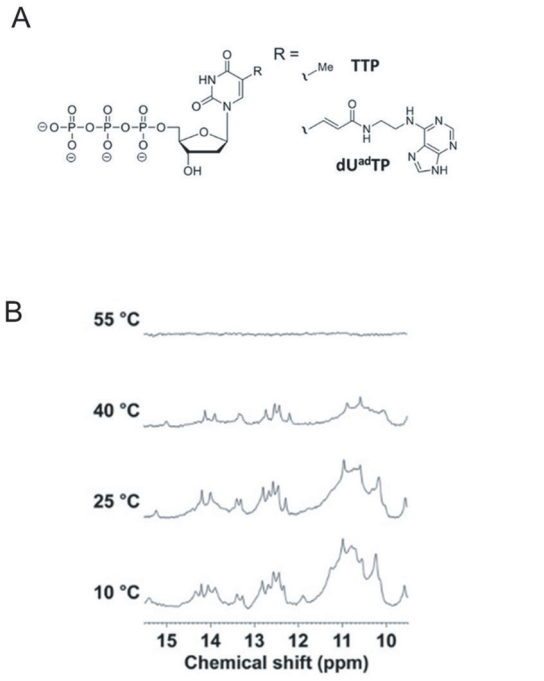

Figure 2. Imino proton spectra of the salivary α-amylase aptamer containing dUad. (A) Chemical structures of natural TTP and dUadTP. (B) Imino proton spectra of the salivary α-amylase aptamer recorded at different temperatures between 10 °C and 55 °C. Reproduced from Minagawa et al (2017) with permission. Copyright 2017 Nature Publishing Group.

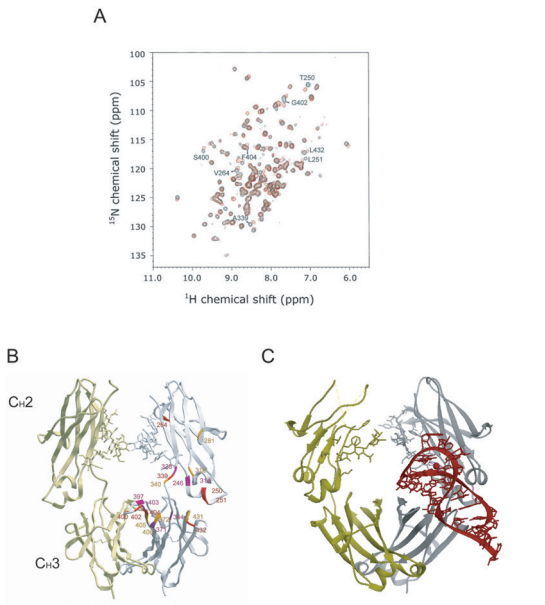

Figure 3. Interaction analysis between the Fc fragment of IgG and its aptamer. (A) Superposition of the 1H-15N HSQC spectra of the 15N-G, I, L, K, T, V, A, M, C, H, W, Y, F, S-labelled Fc fragment (black) and that of the aptamer-bound Fc fragment (red). Relevant amino acid positions are assigned. (B) Mapping of the amino acid residues perturbed upon aptamer addition on the crystal structure of the IgG Fc fragment. Amino acids showing NMR chemical shifts upon aptamer binding are indicated in red for large shifts, orange for medium shifts, and purple for residues that were perturbed but not quantitatively assigned due to overlap or line broadening of the signals. The assigned residues are marked only on one strand of the IgG Fc fragment for clarity. (C) Crystal structure of the aptamer-IgG Fc fragment complex. The aptamer is shown in red. Panels A and B are reproduced from Miyakawa et al (2008) with permission. Copyright 2008 RNA Society. Panel C was generated using UCSF Chimera (Pettersen et al, 2004).

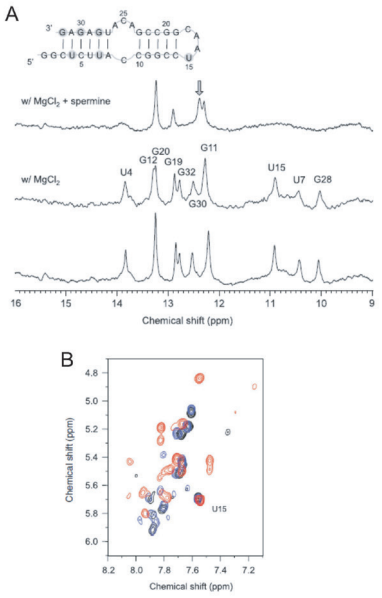

Figure 4. NMR spectra of the spermine aptamer. (A) Imino proton spectra of the aptamer. Bottom: spectrum of the aptamer; middle: spectrum of the aptamer in the presence of 1mM MgCl2; top: spectrum of the aptamer in the presence of 1mM MgCl2 and 5mM spermine. Assignment is indicated on the middle spectrum. Positions of disappeared signals are shaded in the secondary structure. Arrow indicates the resonance that appeared in the presence of spermine. (B) TOCSY spectra of the aptamer (black), in the presence of 1mM MgCl2 (blue), and 1mM spermine with MgCl2 (red). Reproduced from Oguro et al (2016) with the permission of Oxford University Press.

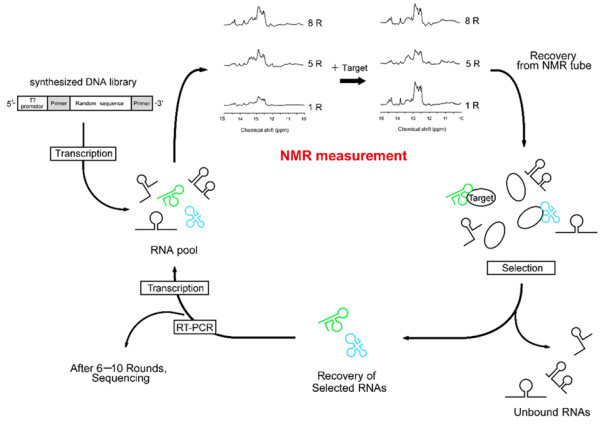

Figure 5. NMR monitoring of the SELEX process. Imino proton signals of RNA pools and RNA binding to target proteins are monitored by NMR and then subjected to selection. The addition of target molecules can be skipped. Reproduced from Amano et al (2017) with permission. Copyright 2017 Nature Publishing Group.

spectra of the ^{15}N-labelled Fc fragment in which some signals were perturbed upon aptamer binding. The perturbed residues are shown in red on the crystal structure of the Fc fragment in Figure 3B, and the binding surface, confirmed by X-ray crystallography, is shown in Figure 3C (Nomura et al, 2010).

Changes in imino proton signals are often used in interaction analyses. Figure 4A shows the imino proton spectra of a spermine-binding aptamer in the absence and presence of spermine (Oguro et al, 2016). Although the addition of Mg^{2+} did not affect the spectrum, a drastic change was observed upon the addition of spermine. The broadening and disappearance of the signals of the terminal stem suggested that the base pairs of the region opened upon binding of spermine. Perturbations of pyrimidine H5–H6 signals in TOCSY spectra were also observed upon spermine binding, indicating a conformational change (Figure 4B). These chemical shift changes can be mapped onto the secondary structure of the aptamer when the tertiary structure remains to be determined.

PERSPECTIVES

Recently, thermodynamic studies of aptamers using isothermal titration calorimetry (ITC) have been reported (Amano R et al, 2016; Neves MAD et al, 2017; Sakamoto et al, 2017). From ITC measurement, the thermodynamic parameters, including dissociation constant K_d, Gibbs free energy change ΔG, enthalpy change ΔH, entropy change ΔS, and stoichiometry, can be obtained. Thus, the combination of NMR and ITC could provide information about the mechanisms of the high-affinity binding of aptamers to their targets. Neves and colleagues revealed that a cocaine-

binding aptamer binds two molecules of its ligand in buffer conditions of low NaCl concentration using ITC. Finally, they showed the location of the binding site using NMR. Moreover, in-cell NMR has been developed to obtain information on the structure, dynamics and interaction of proteins and nucleic acids in living cells (Bao H-L et al, 2017; Yamaoki et al, 2017). Therefore, in-cell NMR may represent a promising approach in the analysis of the structure–function relationship of aptamers in living cells.

The use of NMR spectroscopy to monitor the enrichment of aptamers during SELEX has been reported (Amano et al, 2017). NMR monitoring is simpler and faster than surface plasmon resonance (SPR) or high-throughput sequencing (HTS), which are usually used for monitoring the SELEX process. While SPR and HTS require 2–3 days for sample preparation and 1 day for measurement, a 1D imino proton spectrum of an RNA pool can be measured within 1 or 2hr without extra sample preparation (Figure 5). RNA pools can be used for NMR measurement following transcription and purification. The RNA pools can then be recovered and directly used for selection. Furthermore, target binding of the pool can be analysed during monitoring by addition of the target to the NMR tube. Further development of the NMR monitoring method would enhance the efficiency of aptamer development.

CONCLUSIONS

Since the 1990s, NMR has been used to study aptamer structures and aptamer–target interactions. NMR studies have revealed that aptamers adopt characteristic conformations and bind to their targets. Furthermore, even when it has not been possible to determine the structure, NMR has provided abundant information about the conformations and binding properties of aptamers. Recently, the sensitivity of NMR has been improved and new techniques to obtain new information of samples have been developed (Barnwal et al, 2017; LeBlanc et al, 2017; Nußbaumer et al, 2017). NMR will contribute more to the development of aptamers in the future.

ACKNOWLEDGEMENTS

I sincerely thank all my current and former students, and post-doctoral fellows and colleagues who participated in the aptamer studies in my laboratory.

COMPETING INTERESTS

None declared.

LIST OF ABBREVIATIONS

NMR: **N**uclear **M**agnetic **R**esonance
SELEX: **S**ystematic **E**volution of **L**igands by **EX**ponential enrichment
ATP: **A**denosine-5′-**T**ri**P**hosphate
FMN: **F**lavin **M**ono**N**ucleotide
dU^{ad}TP: (*E*)-5-(2-(*N*-(2-(N6-**ad**eninyl)ethyl))carbamylvinyl)-2′-**d**eoxy**U**ridine-5′-**T**ri**P**hosphate
TTP: **T**hymidine-5′-**T**ri**P**hosphate
IgG: **I**mmuno**g**lobulin **G**
Fc: **F**ragment **c**rystallizable
HSQC: **H**eteronuclear **S**ingle **Q**uantum **C**oherence
TOCSY: **TO**tally **C**orrelated **S**pectroscop**Y**
ITC: **I**sothermal **T**itration **C**alorimetry
SPR: **S**urface **P**lasmon **R**esonance
HTS: **H**igh **T**hroughput **S**equencing.

REFERENCES

Amano R, Aoki K, Miyakawa S, et al. 2017. NMR monitoring of the SELEX process to confirm enrichment of structured RNA. Sci Reports, 7, 283.
Amano R, Takada K, Tanaka Y, et al. 2016. Kinetic and thermodynamic analyses of interaction between a high-affinity RNA aptamer and its target protein. Biochemistry, 55, 6221-6229.
Bao H-L, Ishizuka T, Sakamoto T, et al. 2017. Characterization of human telomere RNA G-quadruplex structures in vitro and in living cells using ^{19}F NMR spectroscopy. Nucleic Acids Res, 45, 5501-5511.
Baouendi M, Cognet JA, Ferreira CS, et al. 2012. Solution structure of a truncated anti-MUC1 DNA aptamer determined by mesoscale modeling and NMR. FEBS J, 279, 479-490.
Barnwal RP, Yang F and Varani G. 2017. Applications of NMR to structure determination of RNAs large and small. Arch Biochem Biophys, 628, 42-56.
Bjerregaard N, Andreasen PA and Dupont DM. 2016. Expected and unexpected features of protein-binding RNA aptamers. WIREs RNA, 7, 744-757.
Carothers JM, Davis JH, Chou JJ and Szostak JW. Solution structure of an informationally complex high-affinity RNA aptamer to GTP. RNA, 12, 567-579.
Chayen NE and Saridakis E. 2008. Protein crystallization: From purified protein to diffraction-quality crystal. Nat Methods, 5, 147-153.
Churcher ZR, Neves MAD, Hunter HN and Johnson PE. 2017. Comparison of the free and ligand-bound imino hydrogen exchange rates for the cocaine-binding aptamer. J Biomol NMR, 68, 33-39.
Darmostuk M, Rimpelova S, Gbelcova H and Ruml T. 2015. Current approaches in SELEX: an update to aptamer selection technology. Biotechnol Adv, 33, 1141-1161.
Davlieva M, Donarski J, Wang J, Shamoo Y, Nikonowicz EP. 2014. Structure analysis of free and bound states of an RNA aptamer against ribosomal protein S8 from Bacillus anthracis. Nucleic Acids Res, 42, 10795-10808.
Dieckmann T, Suzuki E, Nakamura GK and Feigon J. 1996. Solution structure of an ATP-binding RNA aptamer reveals a novel fold. RNA, 2, 628-40.
Fan P, Suri AK, Fiala R, Live D and Patel DJ. 1996. Molecular recognition in the FMN-RNA aptamer complex._J Mol Biol, 258, 480-500.
Flinders J, DeFina SC, Brackett DM, Baugh C, Wilson C and Dieckmann T. 2004. Recognition of planar and nonplanar ligands in the malachite green-RNA aptamer complex. Chembiochem, 5, 62-72.
Gelinas AD, Davies DR and Janjic N. 2016. Embracing proteins: structural themes in aptamer-protein complexes. Curr Opin Struct Biol, 36, 122-132.
Huang DB, Vu D, Cassiday LA, Zimmerman JM, Maher LJ III and Ghosh G. 2003 Crystal structure of NF-kB (p50)2 complexed to a high-affinity RNA aptamer. Proc Natl Acad Sci USA, 100, 9268-9273.
Jiang F, Gorin A, Hu W, et al. 1999. Anchoring an extended HTLV-1 Rex peptide within an RNA major groove containing junctional base triples. Structure, 7, 1461-1472.
Jiang F, Kumar RA, Jones RA and Patel DJ. 1996. Structural basis of RNA folding and recognition in an AMP-RNA aptamer complex. Nature, 382, 183-186.
Jiang L, Majumdar A, Hu W, Jaishree TJ, Xu W and Patel DJ. 1999. Saccharide-RNA recognition in a complex formed between neomycin B and an RNA aptamer. Structure, 7, 817-827.

Jiang L, Suri AK, Fiala R and Patel DJ. 1997. Saccharide-RNA recognition in an aminoglycoside antibiotic-RNA aptamer complex. Chem Biol, 4, 35-50.

Kim YB, Wacker A, Laer KV, Rogov VV, Suess B and Schwalbe H. 2017. Ligand binding to 2′-deoxyguanosine sensing riboswitch in metabolic context. Nucleic Acids Res, 45, 5375-5386.

Lebars I, Richard T, Di Primo C and Toulmé JJ. 2007. NMR structure of a kissing complex formed between the TAR RNA element of HIV-1 and a LNA-modified aptamer. Nucleic Acids Res, 35, 6103-6114.

LeBlanc RM, Longhini AP, Le Grice SFJ, Johnson BA and Dayie TK. 2017. Combining asymmetric ^{13}C-labeling and isotopic filter/edit NOESY: a novel strategy for rapid and logical RNA resonance assignment. Nucleic Acids Res, 45, e146.

Lietard J, Abou Assi H, Gómez-Pinto I, González C, Somoza MM and Damha MJ. 2017. Mapping the affinity landscape of Thrombin-binding aptamers on 2′F-ANA/DNA chimeric G-Quadruplex microarrays. Nucleic Acids Res, 45, 1619-1632.

Lin CH and Patel DJ. 1996. Encapsulating an amino acid in a DNA fold. Nat Struct Biol, 3, 1046-1050.

Lin CH, Wang W, Jones RA and Patel DJ. 1998. Formation of an amino-acid-binding pocket through adaptive zippering-up of a large DNA hairpin loop. Chem Biol, 5, 555-572.

Marathias VM, Wang KY, Kumar S, Pham TQ, Swaminathan S and Bolton PH. 1996. Determination of the number and location of the manganese binding sites of DNA quadruplexes in solution by EPR and NMR in the presence and absence of thrombin. J Mol Biol, 260, 378-394.

Marušič M, Veedu RN, Wengel J and Plavec J. 2013. G-rich VEGF aptamer with locked and unlocked nucleic acid modifications exhibits a unique G-quadruplex fold. Nucleic Acids Res, 41, 9524-9536.

Mashima T, Matsugami A, Nishikawa F, Nishikawa S, Katahira M. 2009. Unique quadruplex structure and interaction of an RNA aptamer against bovine prion protein. Nucleic Acids Res, 37, 6249-6258.

Mashima T, Nishikawa F, Kamatari YO, et al. 2013. Anti-prion activity of an RNA aptamer and its structural basis. Nucleic Acids Res, 41, 1355-1362.

Matsugami A, Kobayashi S, Ouhashi K, et al. 2003. Structural basis of the highly efficient trapping of the HIV Tat protein by an RNA aptamer. Structure, 11, 533-545.

Minagawa H, Onodera K, Fujita H, et al. 2017. Selection, characterization and application of artificial DNA aptamer containing appended bases with sub-nanomolar affinity for a salivary biomarker. Sci Reports, 7, 42716.

Miyakawa S, Nomura Y, Sakamoto T, et al. 2008. Structural and molecular basis for hyperspecificity of RNA aptamer to human immunoglobulin G. RNA, 14, 1154-1163.

Neves MAD, Slavkovic S, Churcher ZR and Johnson PE. 2017. Salt-mediated two-site binding by the cocaine-binding aptamer. Nucleic Acids Res, 45, 1041-1048.

Nomura Y, Fukunaga J, Tanaka Y, et al. 2013. Solution structure of a DNA mimicking motif of an RNA aptamer against transcription factor AML1 Runt domain. J Biochem, 154, 513-519.

Nomura Y, Sugiyama S, Sakamoto T, et al. 2010. Conformational plasticity of RNA for target recognition as revealed by the 2.15 Å crystal structure of a human IgG-aptamer complex, Nucleic Acids Res, 38, 7822-7829.

Nußbaumer F, Juen MA, Gasser C, Kremser J, Müller T, Tollinger M and Kreutz C. 2017. Synthesis and incorporation of 13C-labeled DNA building blocks to probe structural dynamics of DNA by NMR. Nucleic Acids Res, 45, 9178-9192.

Oguro A, Yanagida A, Fujieda Y, et al. 2016. Two stems with different characteristics and an internal loop in an RNA aptamer contribute to spermine-binding. J Biochem, 161, 197-206.

Pettersen EF, Goddard TD, Huang CC, et al. 2004. UCSF Chimera--a visualization system for exploratory research and analysis. J Comput Chem, 25, 1605-1612.

Reiter NJ, Maher LJ and Butcher SE. 2008. DNA mimicry by a high-affinity anti-NF-kB RNA aptamer. Nucleic Acids Res, 36, 1227-1236.

Robertson SA, Harada K, Frankel AD and Wemmer DE. 2000. Structure determination and binding kinetics of a DNA aptamer-argininamide complex. Biochemistry, 39, 946-954.

Sakamoto T, Ennifar E and Nakamura Y. 2017. Thermodynamic study of aptamers binding to their target proteins. Biochimie, DOI: 10.1016/j.biochi.2017.10.010.

Sakamoto T, Oguro A, Kawai G, Ohtsu T and Nakamura Y. 2005. NMR structures of double loops of an RNA aptamer against mammalian initiation factor 4A. Nucleic Acids Res, 33, 745-754.

Schultze P, Macaya RF and Feigon J. 1994. Three-dimensional solution structure of the thrombin-binding DNA aptamer d(GGTTGGTGTGGTTGG). J Mol Biol, 235, 1532-1547.

Van Melckebeke H, Devany M, Di Primo C, et al. 2008. Liquid-crystal NMR structure of HIV TAR RNA bound to its SELEX RNA aptamer reveals the origins of the high stability of the complex. Proc Natl Acad Sci USA, 105, 9210-9215.

Wolter AC, Weickhmann AK, Nasiri AH,et al. 2017. A Stably Protonated Adenine Nucleotide with a Highly Shifted pK_a Value Stabilizes the Tertiary Structure of a GTP-Binding RNA Aptamer. Angew Chem Int Ed Engl, 56, 401-404.

Yamaoki Y, Kiyoishi A, Miyake M, et al. 2017. The first successful observation of in-cell NMR signals of DNA and RNA in living human cells. Phys Chem Chem Phys, DOI: 10.1039/c7cp05188c.

Yang Y, Kochoyan M, Burgstaller P, Westhof E and Famulok M. 1996. Structural basis of ligand discrimination by two related RNA aptamers resolved by NMR spectroscopy. Science, 272, 1343-1347.

Ye X, Gorin A, Ellington AD and Patel DJ. 1996. Deep penetration of an alpha-helix into a widened RNA major groove in the HIV-1 rev peptide-RNA aptamer complex. Nat Struct Biol, 3, 1026-1033.